

4.4 EXPERIMENTAL DATA OF AEROSOL PARTICLE AND CLOUD PROPERTIES FOR WARM, COLD AND MIXED-PHASE CLOUDS IN COMPARISON WITH MODELING RESULTS

Silvia Henning¹, Ernest Weingartner¹, Sabine Wurzler², Karoline Diehl² and Urs Baltensperger^{1*}

¹Paul Scherrer Institut, CH-5232 Villigen PSI, Switzerland.

²Institute for Tropospheric Research, DE-04303 Leipzig, Germany.

1. INTRODUCTION

During several field campaigns (e.g. Winter 2000 & Summer 2000) the interstitial and total aerosol particle size distributions as well as the cloud particle size distribution and the water content (*LWC*) of clouds were measured at the high-alpine research station Jungfrauoch (3580 m asl, Switzerland). With a cloud frequency of about 40% the site is highly suitable for in-situ aerosol particle and cloud measurements.

2. EXPERIMENTAL

Aerosol number size distributions of the total and the interstitial aerosol were measured with a Scanning Mobility Particle Sizer (SMPS, particle diameter $D_p = 18 - 800$ nm). A Forward Scattering Spectrometer Probe (FSSP-100, Particle Measuring Systems Inc., USA) was operated to detect the cloud droplet size distribution, and a Particle Volume Monitor (PVM-100, Gerber Scientific Inc., USA) measured the liquid water content *LWC*. In addition, measurements of the chemical aerosol composition were performed in two size classes (total suspended particulate matter (TSP) and particles with an aerodynamic diameter less than $1 \mu\text{m}$ (PM_{10})), of the total aerosol. In addition, data from other instruments continuously operated at the JFJ in the framework of the Global Atmosphere Watch (GAW) Program (Nyeki et al., 1998) were available, as well as data from continuous meteorological measurements (wind direction, wind velocity, air pressure, air temperature, relative humidity, solar radiation) from the Swiss Meteorological Institute (MeteoSwiss) and the mass of total suspended particulate matter (TSP) from the Swiss National Monitoring Network for Air Pollutants (NABEL).

2.1 Description of the JFJ measurement site

The high-alpine research station JFJ (3580 m asl; $46^{\circ}33'N$, $7^{\circ}59'E$, Switzerland) is part of the GAW Program of the World Meteorological

Organization, since it is an ideal site to investigate the chemistry and physics of the free troposphere above a continental region. More information about the site is found in Baltensperger et al. (1997).

2.2 The inlet systems

Aerosol particles were sampled from two different inlet systems. The total aerosol inlet is heated to $+20^{\circ}\text{C}$ and is designed to evaporate all cloud droplets at an early stage of the sampling process. Calculations for this set-up showed that activated droplets smaller than $40 \mu\text{m}$ can be sampled up to a wind speed of 20 m s^{-1} (Weingartner et al., 1999). The total sample thus consists of aerosols activated to cloud droplets, aerosols scavenged by droplets, and inactivated (interstitial) aerosols. The second inlet system was designed to only sample interstitial aerosols. Two different inlet types were used. In summer, an aerodynamic size discriminator (Round Jet Impactor, RJI) operating at ambient temperature (i.e. without any heating) was used. This device is a conventional impactor where particles larger than the cut-off size are unable to follow the airflow streamlines and hence impact onto a plate. The cut-off size is given by the slit width of the impactor and the flow rate. In our setup an impactor with a cut-off diameter at $5 \mu\text{m}$ was used as the interstitial aerosol inlet. Once a day sampling was interrupted and the inlet was cleaned and dried. In winter a different inlet design was operated, since the RJI was expected to suffer from freezing. Therefore, the upper stages of a cascade impactor (Maenhaut et al., 1996b) with a size cut of $1 \mu\text{m}$ were used for the separation of interstitial aerosol and activated particles.

2.3 Measurement of Aerosol Size Distributions

The atmospheric aerosol was fed into the building (indoor $T = 20$ to 30°C , $\text{RH} < 10\%$) from either the total inlet or the interstitial inlet using two 2-way pinch-valves, and then on to a single SMPS (scanning mobility particle sizer) system for measurement of the size distribution. The SMPS consisted of a differential mobility analyzer (DMA, TSI 3934), a bipolar charger to obtain charge equilibrium (krypton source, ^{85}Kr) and a condensation particle counter (CPC, TSI

*Corresponding author address: U. Baltensperger, Paul Scherrer Institut, CH-5232 Villigen PSI, Switzerland. Email: urs.baltensperger@psi.ch

3022A). The poly- and monodisperse flow was 0.3 l min^{-1} while sheath and excess air flows (3 l min^{-1}) were operated in a closed-loop system. The excess air outlet of the DMA was fixed to the vacuum side of the pump, while the air exiting the pump was cleaned from particles by a filter and used as sheath air. The flow was held constant by a critical orifice positioned before the pump.

With this set-up the aerosol size distribution from $D_p = 18 \text{ nm}$ to 800 nm was measured at an average ambient pressure of 650 hPa . Scanning was performed in logarithmically equidistant steps with a time resolution of about 6 minutes per scan (300 seconds up scan time, 10 seconds down scan and 60 seconds wait time while the inlet line was switched, resulting in a scanning velocity of $d\log D/dt = 5.7 \cdot 10^{-3} \text{ s}^{-1}$). With this scanning velocity no deformation of the size distribution occurs (Weingartner et al., 2002). The scanning time was synchronized with the time of the pinch valve. For further data processing one-hour averages of the interstitial and total particle size distributions were calculated.

2.4 Calibration of the SMPS system

To make sure that the aerosol size distribution was not biased by diffusion and impaction losses in the 2-way pinch valves, tests with monodisperse latex spheres (nominal diameters of $91 \pm 6 \text{ nm}$ and $550 \pm 5 \text{ nm}$) were performed. A latex solution was nebulized, and the droplets were dried in a diffusion dryer. The particle number concentrations of the monodisperse size distributions were measured before and after passing the pinch valve. The calculated deviations of the particle number concentration between the different lines were of the same order of magnitude as the inter-variance of the original aerosol size distributions. For the 91 nm latex spheres the deviation at the maximum of the distribution was 9% and the variance was calculated to be 7%, while for the 550 nm latex spheres values of 6% and 5% were found, respectively. Based on these results the influence of the 2-way pinch valve on particles losses can be neglected.

This experimental setup was also used to check the voltage to diameter adjustment and the delay time of the SMPS. The measured particle size distributions were fitted with a lognormal function. For the 91 nm polystyrene particles a diameter of 90 nm with a half-width of 8 nm was determined. A diameter of 556 nm with a half-width of 80 nm was found for the 550 nm spheres.

With a slightly different experimental set-up, where a particle filter was included in one line

and ambient air was measured in the other path, it was shown that the waiting time of 60 seconds between two scans was sufficient to flush all particles from the previous scan out of the inlet system.

2.5 Instrumentation for measuring cloud microphysics

A PVM-100 (Gerber, 1991) was used to measure total *LWC* during the experiment. It measures the light scattered by a cloud droplet population exposed to a laser beam and relates it to the *LWC*. It was situated outside the building on the rail of the upper platform of the building. The optics of the PVM-100 were cleaned just before the experiment, secondary calibration was conducted regularly (typically every cloud free day) as suggested by the manufacturer.

The FSSP-100 situated 2 m away from the PVM-100, was used for measuring cloud droplet size distributions in the droplet diameter range between either 4.5 and $30 \mu\text{m}$ or 6.3 and $62 \mu\text{m}$. In difference to the PVM, the FSSP sizes the single droplets one by one. The droplets are passed through a laser beam corresponding to the amount of light scattered by the drops in the forward direction. A description of this probe can be found in Knollenberg (1981). For ground-based measurements, air is actively sucked into the sampling tube to provide a constant droplet stream and a well defined sample volume.

Dye and Baumgardner (1984) and Cerni (1983) report on systematic errors of the instrument which can be divided into two types: (a) Under- or oversizing of droplets due to varying opto-electronical setup, and (b) Counting losses caused by coincidences (when there are two or more droplets simultaneously in the laser beam) and by the electronic dead-time. To correct for sizing uncertainties, calibration with monodisperse glass beads was conducted before, during, and after the campaign. Counting losses were compensated by multiplying the measured concentrations with the half-empirical correction factor $1/(1-mA)$ proposed by Baumgardner et al. (1985), where A is the measured activity, i.e. the fraction of time the probe was active processing droplet data. The parameter m was considered to be constant and set to 0.73 as proposed by the manufacturer. In addition, the concentration was corrected for a varying velocity acceptance ratio (Wendisch, 1998), which was simultaneously measured. A comparison of different correction schemes for concentration measurements with the FSSP is given by Brenguier (1989).

Wind ramming (Choulaton et al., 1986) alters the droplet velocity, and hence changes the sample volume and the droplet concentration.

However, this possible bias could not be corrected as wind sensors next to the instrument were not available. Laser beam inhomogeneities (Baumgardner and Spowart, 1990) which systematically broaden the measured droplet size distribution measured with an FSSP (Wendisch et al., 1996), were not considered because the laser beam cross section intensity profile is not sufficiently stable.

The droplet number concentration N_i ($i=1, \dots, 15$, denotes the channel number) for each of the FSSP size channels is obtained by dividing the raw counts in the 15 size classes by the sampled air volume. The total droplet concentration N_D is obtained by summing up over all size classes. The *LWC* and the effective radius (R_{eff}) are defined as:

$$LWC = \frac{\pi}{6} \rho_w \sum_{i=1}^{15} N_i D_i^3 \quad (1)$$

$$R_{\text{eff}} = \frac{1}{2} \sum_{i=1}^{15} N_i D_i^3 / \sum_{i=1}^{15} N_i D_i^2 \quad (2)$$

where ρ_w is the density of water and D_i are the center droplet diameters in each size channel i , attributed by the size calibration. The corrected droplet size distribution is obtained by dividing the droplet number concentration N_i by the width of the respective size channel.

The *LWC*, calculated from the corrected FSSP data (Eq. 1), were compared to the *LWC* directly measured by the PVM, which revealed the following correlation equation (correlation coefficient R^2 of 0.81):

$$LWC(FSSP) = LWC(PVM) * 1.484 - 0.009 \text{ g m}^{-3} \quad (3)$$

The systematic underestimation of the *LWC* by the PVM may be a result of decreasing sensitivity of the PVM with increasing droplet diameter as reported by Arends et al. (1992), Wendisch et al. (1998) and Wendisch (1998), but may also be explained by a varying sample volume of the FSSP. Wind tunnel tests of the airborne version of the PVM (the PVM-100A) have also shown a decreasing sensitivity of the PVM with increasing droplet diameter (Wendisch et al., 2000). In the results section the *LWC* measured by the PVM was used, if not mentioned otherwise.

Water saturation data of the air mass were obtained with a Thygan (VTP 6) instrument, which is used in the regular network (ANETZ) of MeteoSwiss (Dössegger et al., 1992). This instrument is designed to determine reliable relative humidity data at sites with harsh weather conditions. It is a ventilated, heated thermometer, combined with a dew point

hygrometer, with an accuracy of $\pm 0.15^\circ\text{C}$ in the observed temperature range. Because of the complex topographical situation at the Jungfraujoch two instruments were used, one on the south side and one on the north side of the measuring site.

2.6 Chemical aerosol analysis

In addition to aerosol physical properties, filter samples in two size classes (total suspended particles, TSP and particles with $D_p < 1 \mu\text{m}$, PM_{10}) for aerosol chemical analysis were obtained at the total aerosol inlet. The cut-off of $1 \mu\text{m}$ was achieved by using the first 5 stages of the 12-stage impactor developed by Maenhaut et al. (1996a). The flow was held constant at 11 l min^{-1} by a mass flow controller, which yielded the desired cut-off diameter of $1 \mu\text{m}$ for the PM_{10} line. The aerosol was sampled on filter packs consisting of a Teflon (Sartorius, Microfilter PTFE; $1.2 \mu\text{m}$ pore diameter) and a Nylon (Gelman, Nylasorb, $1.0 \mu\text{m}$ pore diameter) filter. This type of set-up was chosen to catch semi-volatile nitrate aerosol material on the nylon filter, which evaporated from the Teflon filter. The sampling interval was 24 hours during the whole campaign.

The samples were stored at temperatures around -8°C and were analyzed for water soluble major anions and cations by ion chromatography shortly after the campaign.

3 RESULTS

From the total and interstitial aerosol particle size distributions the size resolved activation of the aerosol particles was calculated according to:

$$F_N(D_p) = \frac{(N_{\text{tot}}(D_p) - N_{\text{int}}(D_p))}{N_{\text{tot}}(D_p)} \quad (4)$$

where F_N is the scavenging ratio, D_p the particle diameter, and N_{tot} , N_{int} are total and interstitial particle number concentration, respectively, at a given D_p .

In Fig. 1, typical examples of the scavenging ratio are given as a function of the particle diameter for three different scenarios, one during the summer campaign and two during the winter campaign. During the summer campaign, the temperature ranged between -7°C and $+5^\circ\text{C}$, and during the winter campaign between -24°C and -5°C . The scenarios were one rather warm summer cloud, one moderately cold winter cloud and one cold winter cloud. The data in Figure 1 are averaged over 3 days in summer (scenario 1, see below) and over 1 day in winter (scenarios 2 and 3).

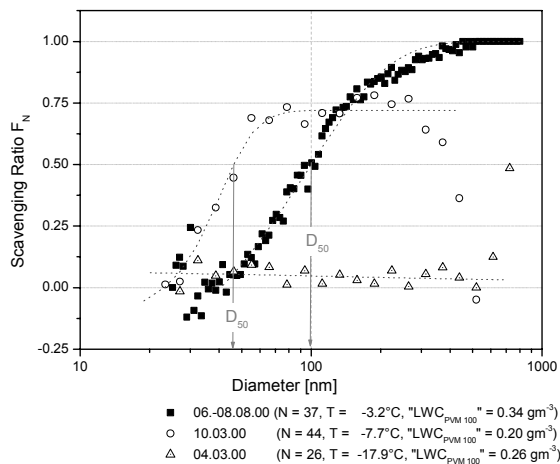


Figure 1. Size resolved scavenging ratios of the aerosol for 3 examples, a warm water cloud (6 to 8 August 2000, black squares), a mixed phase cloud (10 March 2000, open circles) and an ice cloud (4 March 2000, triangles).

Scenario 1: The black squares in Fig. 1 represent a summer cloud with a mean temperature of -3.2°C and a LWC of 0.34 g m^{-3} . The Thygan data indicate a supersaturation of the cloud with respect to water. The scavenging curve shows a typical S-shape, which was also observed by other authors (Martinsson et al., 1999). One can notice from the curve that total activation was reached for particles larger than 400 nm, and the diameter of 50% activation (D_{50}) was around 100 nm. Similar values for D_{50} were obtained for all summer clouds but only for cases where $LWC > 0.15\text{ g m}^{-3}$ (Henning et al., 2002). Furthermore, a decrease of the effective radius of cloud droplets (R_{eff}) with increasing $N_{\text{tot}, D_p > 100}$ was observed, providing experimental evidence for the microphysical relation predicted by the Twomey effect (Twomey, 1974; 1977).

Scenario 2: The open circles represent a winter cloud with a mean temperature of -7.7°C and a LWC of 0.20 g m^{-3} . This moderately cold winter cloud was supersaturated with respect to ice, but not with respect to water. The scavenging curve shows the same feature as the one for the summer cloud. However, even though D_{50} was found to be around 45 nm, i.e., significantly smaller than for the summer clouds, the activation rate of the aerosol particles did not exceed 75%. On the contrary, for particles larger than 300 nm the activation rate decreases again.

Scenario 3: The triangles in Fig. 1 represent a cold winter cloud with a mean temperature of -17.9°C and an apparent LWC of 0.26 g m^{-3} . This cloud was hardly saturated with respect to ice and not at all with respect to water. In this case, the scavenging curve was significantly different, i.e., a rather flat line with values near zero, indicating nearly no activation of particles.

Only for particle sizes larger than 500 nm an increase of the activation ratio was found.

A possible explanation of the finding that the winter clouds showed less activation of the aerosol particles might be that they contained ice particles as well as supercooled droplets. If the actual saturation in the cloud was higher than the saturation with regard to ice but lower than the saturation with regard to water the ice particles would have grown at the expense of the droplets according to the Bergeron-Findeisen process (Pruppacher and Klett, 1980). By this way, interstitial aerosol particles are released by the evaporation of water droplets. As mentioned above, this was the case for the moderately cold winter cloud but even more so for the cold winter cloud. In the latter case saturation with respect to ice was hardly reached which explains the very low number of activated aerosol particles. The enhancement of the activation rate of the cold winter cloud for larger particles might be explained by the increasing efficiency of aerosol particles to act as ice nuclei for particles larger than 200 nm in diameter (Pruppacher and Klett, 1980).

4. MICROPHYSICAL EXPLANATION

Scenario 1: summer cloud

In the summer cloud the mean temperature was -3.2°C , and the actual saturation showed values around saturation with regard to water. Assuming that the cloud did not experience lower temperatures than the measured ones ice formation will be rather unlikely. The only ice forming process which might take place at that rather warm temperature is contact freezing by only two insoluble species, i.e. montmorillonite particles (Pitter and Pruppacher, 1973) or bacteria (Levin and Yankofsky, 1983). However, this would be rather unlikely to take place. Therefore, we may conclude that a mere water cloud was present.

Scenario 3: cold winter cloud

In this cloud the mean temperature was -17.9°C , and the actual saturation was slightly higher than saturation with regard to ice but lower than saturation with regard to water. Considering the temperature, saturation and scavenging feature this cloud was probably an ice cloud containing only small ice crystals grown by water vapor deposition. Therefore, the LWC given by the PVM instrument is believed to be biased by the ice content. According to the temperature the form of the ice crystals can be assumed (Pruppacher and Klett, 1980). At a

temperature of -18°C thick ice plates are expected with a size of about 1 mm.

Scenario 2: moderately cold winter cloud

In this cloud the mean temperature was -5.7°C , and the actual saturation was between saturation with regard to ice and saturation with regard to water. Based on these data we can assume a mixed population of supercooled droplets, rimed ice crystals and probably column shaped ice crystals. Frozen drops can hardly be expected. Immersion freezing, which would be possible at the mentioned temperatures, will work only for rather large drops of around 200 μm in diameter (for model description see Diehl and Wurzler (2002)). Contact freezing can take place at these temperatures by several mineral particles (Pitter and Pruppacher, 1973) as well as by several biological particles (Schnell and Vali, 1976; Levin and Yankofsky, 1983; Diehl and Wurzler, 2002) but will still be rather unlikely to take place.

5. CONCLUSIONS

Combining the field observations with model calculations, we conclude that:

1. The summer clouds consisted only of water drops, because the temperatures were too warm for ice formation. Therefore, the scavenging curve can be assumed as typical for warm clouds.
2. According to the microphysical data, the winter clouds were mixed-phase clouds for temperatures between -5°C and -12°C , consisting of supercooled droplets, ice crystals, and rimed ice particles. Under these conditions, droplets may evaporate in order to compensate for the water vapor deposition to the ice crystals. This process (called the Bergeron-Findeisen-process) is due to a different saturation vapor pressure over ice and droplets and may result in an increase of the interstitial aerosol fraction, which in turn will yield a scavenging ratio below 1.
3. The winter clouds observed at temperatures below -12°C consisted nearly exclusively of ice crystals, as indicated by the microphysical data. This cloud can possibly be regarded as an aged mixed-phase cloud, where after sufficiently long time all the liquid water was evaporated, due to the Bergeron-Findeisen-process. Further analysis is on going in order to verify this hypothesis.

6. ACKNOWLEDGMENTS

We thank the International Foundation High Altitude Research Stations Jungfrauoch and Gornergrat (HFSJG), which made it possible for us to carry out our experiments at the High Altitude Research Station at Jungfrauoch. The financial support of MeteoSwiss (Global Atmosphere Watch) is highly appreciated. We thank S. Schmidt and M. Wendisch (IfT Leipzig) for their help in obtaining the cloud droplet spectra.

7. REFERENCES

- Arends, B. G., G. P. A. Kos, W. Wobrock, D. Schell, K. Noone, S. Fuzzi, and S. Pahl, 1992: Comparison of techniques for measurements of fog liquid water content. *Tellus*, **44B**, 604-611.
- Baltensperger, U., H. W. Gäggeler, D. T. Jost, M. Lugauer, M. Schwikowski, E. Weingartner, and P. Seibert, 1997: Aerosol climatology at the high-alpine site Jungfrauoch, Switzerland. *J. Geophys. Res.*, **102**, 19707-19715.
- Baumgardner, D. and M. Spowart, 1990: Evaluation of the Forward Scattering Spectrometer Probe. Part III: Time response and laser inhomogeneity limitations. *J. Atmos. Oceanic Technol.*, **7**, 666-672.
- Baumgardner, D., W. Strapp, and J. E. Dye, 1985: Evaluation of the Forward Scattering Spectrometer Probe. Part II: Corrections for coincidence and dead-time losses. *J. Atmos. Oceanic Technol.*, **2**, 626-632.
- Brenguier, J.-L., 1989: Coincidence and dead-time corrections for particle counters. Part I: A general mathematical formalism. *J. Atmos. Oceanic Technol.*, **6**, 575-584.
- Cerni, T. A., 1983: Determination of the size and concentration of cloud drops with an FSSP. *J. Climate Appl. Meteor.*, **22**, 1346-1355.
- Choullarton, T. W., I. E. Consterdine, B. A. Gardiner, M. Gay, M. K. Hill, J. Latham, and I. M. Stromberg, 1986: Field studies of the optical and microphysical characteristics of clouds enveloping Great Dun Fell. *Quart. J. Roy. Meteorol. Soc.*, **112**, 131-148.
- Diehl, K. and S. Wurzler, 2002: A freezing model for heterogeneous drop freezing in the immersion mode. *J. Atmos. Sci.*, submitted.
- Dössegger, R., G. Haller, B. Hoegger, J. Joss, G. Müller, G. Pilet, P. Wasserfallen, P. Zbinden, and P. Ruppert, 1992: THYGAN Benutzerinformationen und -erfahrungen. *Automatische Messnetze SMA*, Zürich, SMA,

- Arbeitsberichte der Schweizerischen Meteorologischen Anstalt, 60.
- Dye, J. E. and D. Baumgardner, 1984: Evaluation of the Forward Scattering Spectrometer Probe. Part I: Electronic and optical studies. *J. Atmos. Oceanic Technol.*, **1**, 329-344.
- Gerber, H., 1991: Direct measurement of suspended particulate volume concentration and far-infrared extinction coefficient with a laser-diffraction instrument. *Appl. Opt.*, **30**, 4824-4831.
- Henning, S., E. Weingartner, S. Schmidt, M. Wendisch, H. W. Gäggeler, and U. Baltensperger, 2002: Size-dependent aerosol activation at the high-alpine site Jungfraujoch (3580 m asl). *Tellus*, **54B**, 82-95.
- Knollenberg, R. G., 1981: Techniques for probing cloud microstructure. *Clouds, Their Formation, Optical Properties and Effects*, P. V. Hobbs and A. Deepak, Eds., Academic Press, Inc., 15-91.
- Levin, Z. and S. A. Yankofsky, 1983: Contact Versus Immersion Freezing of Freely Suspended Droplets by Bacterial Ice Nuclei. *J. Climate Appl. Meteor.*, **22**, 1964-1966.
- Maenhaut, W., G. Ducastel, C. Leck, E. D. Nilsson, and J. Heintzenberg, 1996a: Multi-elemental composition and sources of the high Arctic atmospheric aerosol during summer and autumn. *Tellus*, **48B**, 300-321.
- Maenhaut, W., R. Hillamo, T. Mäkelä, J. L. Jaffrezo, M. H. Bergin, and C. I. Davidson, 1996b: A new cascade impactor for aerosol sampling with subsequent PIXE analysis. *Nucl. Instr. and Meth. in Phys. Res. B*, **109**, 482-487.
- Martinsson, B. G., G. Frank, S. I. Cederfelt, E. Swietlicki, O. H. Berg, J. C. Zhou, K. N. Bower, C. Bradbury, W. Birmili, F. Stratmann, M. Wendisch, A. Wiedensohler, and B. A. Yuskiewicz, 1999: Droplet nucleation and growth in orographic clouds in relation to the aerosol population. *Atmos. Res.*, **50**, 289-315.
- Nyeki, S., U. Baltensperger, I. Colbeck, D. T. Jost, E. Weingartner, and H. W. Gäggeler, 1998: The Jungfraujoch high-alpine research station (3454 m) as a background clean continental site for the measurement of aerosol parameters. *J. Geophys. Res.*, **103**, 6097-6107.
- Pitter, R. L. and H. R. Pruppacher, 1973: Wind-Tunnel Investigation of Freezing of Small Water Drops Falling at Terminal Velocity in *Air. Quart. J. Roy. Meteorol. Soc.*, **99**, 540-550.
- Pruppacher, H. R. and J. D. Klett, 1980: *Microphysics of clouds and precipitation.*, 714 pp.
- Schnell, R. C. and G. Vali, 1976: Biogenic Ice Nuclei .1. Terrestrial and Marine Sources. *J. Atmos. Sci.*, **33**, 1554-1564.
- Twomey, S., 1974: Pollution and the planetary albedo. *Atmos. Environ.*, **8**, 1251-1256.
- , 1977: The Influence of pollution on the shortwave albedo of clouds. *J. Atmos. Sci.*, **34**, 1149-1152.
- Weingartner, E., S. Nyeki, and U. Baltensperger, 1999: Seasonal and diurnal variation of the aerosol size distributions (10<D<750 nm) at a high-alpine site (Jungfraujoch 3580 m asl). *J. Geophys. Res.*, **104**, 26809-26820.
- Weingartner, E., M. Gysel, and U. Baltensperger, 2002: Hygroscopicity of aerosol particles at low temperatures. 1. New H-TDMA system: Setup and first applications. *Environ. Sci. Technol.*, **36**, 55-62.
- Wendisch, M., 1998: A quantitative comparison of ground-based FSSP and PVM measurements. *J. Atmos. Oceanic Technol.*, **15**, 887-900.
- Wendisch, M., A. Keil, and A. V. Korolev, 1996: FSSP characterization with monodisperse water droplets. *J. Atmos. Oceanic Technol.*, **13**, 1152-1165.
- Wendisch, M., T. Garrett, P. V. Hobbs, and J. W. Strapp, 2000: PVM-100A performance tests in the IRT and NRC wind tunnels. *Proceedings of the 13th International Conference on Clouds and Precipitation*, Reno, USA, 194-197.
- Wendisch, M., S. Mertes, J. Heintzenberg, A. Wiedensohler, D. Schell, W. Wobrock, G. Frank, B. Martinsson, S. Fuzzi, G. Orsi, G. P. A. Kos, and A. Berner, 1998: Drop size distribution and LWC in Po Valley fog. *Contr. Atmos. Phys.*, **71**, 87-100.